

# A MULTI-ANALYTICAL APPROACH FOR CHARACTERIZING PIGMENTS FROM THE TOMB OF *DJEHUTYEMHAB* (TT194), EL- QURNA NECROPOLIS, UPPER EGYPT

## FESTÉKANYAGOK AZONOSÍTÁSA *DJEHUTYEMHAB* (TT194) SÍRJÁBÓL TÖBBFAJTA VIZSGÁLATI MÓDSZER SEGÍTSÉGÉVEL

HUSSEIN HASSAN MAREY MAHMOUD

Department of Conservation, Faculty of Archaeology, Cairo University, 12613 Giza, Egypt

E-mail: [marai79@hotmail.com](mailto:marai79@hotmail.com)

### Abstract

*The present paper aims to characterize some ancient pigments from the painted reliefs of the tomb of Djehutyemhab (TT194), (Ramesside Period, ca. 1298–1064 BC), Nobles tombs, El-Qurna necropolis (Luxor), Upper Egypt. The analytical techniques used in this study were: optical microscopy (OM), scanning electron microscopy (SEM) equipped with an energy dispersive X-ray detector (EDS), X-ray diffraction analysis, micro-Raman and Fourier transform infrared spectroscopies ( $\mu$ -Raman and FT-IR). Based on the results of these analyses, the stratigraphic structure, the morphology and the chemical composition of the paint layers were identified. The results revealed that the blue pigment is Egyptian blue (cuprorivaite,  $\text{CaCuSi}_4\text{O}_{10}$ ), the turquoise-green pigment is Egyptian green (Cu-wollastonite) together with traces of cuprorivaite, the yellow pigment is yellow ochre, and the red pigment is red ochre. Moreover, the preparation layer was identified as a mixture of gypsum and calcite. FT-IR analysis of the paint layers revealed the use of a proteinaceous binder (probably of animal glue). The obtained results will help in establishing a conservation plan of these murals.*

### Kivonat

*A tanulmány célja Djehutyemhab (TT194), (Ramesszida periódus, ca. 1298–1064 BC) sírjából előkerült festékanyagok azonosítása. A sír egy jelentős személyiséghez tartozott, az El-Qurna temetőből került elő (Luxor, Felső Egyiptom). A festékanyagok a sírkamra festett reliefséből származnak. A vizsgálati módszerek a következők voltak: optikai mikroszkópia (OM), szkennelési elektron mikroszkópia (SEM), amelyet energia diszperzív röntgen detektorral szereltek fel (EDS), röntgen diffrakció, mikro-Raman és Fourier transzformációs infravörös spektroszkópia ( $\mu$ -Raman és FT-IR). Ezen vizsgálatok eredményeinek alapján azonosítható volt a festékanyagok rétegtani szerkezete, morfológiája és kémiai összetétele. Az alkalmazott kék szín az ún. egyiptomi kék-nek bizonyult (kalcium-réz-szilikát, kuprorivaite,  $\text{CaCuSi}_4\text{O}_{10}$ ), a türkiz színű festékanyag ún. egyiptomi zöld (Cu-wollastonit) amiben kuprorivaite nyomok is előfordulnak. A sárga színt sárga okkerből nyerték, a vörös szín pedig vörös okkerből származik. Továbbá, az alapozó rétegben gipsz és kalcit keverékét mutattuk ki. A festékrétegek FT-IR vizsgálata szerint fehérje tartalmú kötőanyagot (valószínűleg állati eredetű enyvet) használtak. Az eredmények elősegítik a falfestmények megőrzését és segítenek a megfelelő konzerválási lépések kiválasztásában.*

KEYWORDS: PIGMENTS; EL-QURNA NECROPOLIS; NOBLES TOMBS; SEM-EDS;  $\mu$ -RAMAN; XRD; FT-IR

KULCSSZAVAK: FESTÉKANYAGOK; EL-QURNA TEMETŐ, FŐÜRI SÍROK; SEM-EDS;  $\mu$ -RAMAN; XRD; FT-IR

### Introduction

The ancient city of Thebes is located on the western bank of the Nile River, about 650 km south to Cairo, Egypt. The private or ‘Nobles’ tombs are scattered along the eastern slopes of the Thebes Mountain between the Queen’s Valley and the King’s Valley. There are around five hundred private tombs at least 415 catalogued tombs, signated TT for Theban Tomb belonging to officials of the New Kingdom (c.1570–1070 BC) (Kamil 1976) some of them very simple, the others more complex and beautifully decorated. The

typical Theban tomb type is the [rock-cut tomb](#) and consists of two main parts the subterranean or underground burial chamber, most often undecorated and the decorated chapel accessible for the living. The tomb *Djehutyemhab* (TT194) is located in the necropolis of El-Assasif in Thebes in Egypt, *Djehutyemhab* was an overseer of the marshland-dwellers of the Estate of Amun and a scribe in the temple of Amun during the Nineteenth dynasty of Egypt. This tomb is a part of the TT192 tomb complex (Porter & Moss 1960; Karl-Joachim 1995).

These tombs are carved in the Thebes Mountain (462 meter above present sea-level) composed of marine limestone [lower Eocene] and marls more than 350m thick (Marey Mahmoud 2004). According to Wüst & Schlüchter (2000), the rocks in the Thebes Mountains are composed of carbonate and clay minerals with minor amounts of halite, quartz, gypsum and anhydrite. The lower levels of the Theban Formation are composed of slightly clayey, sub-chalky limestone, which serves to enclose a few bedrock layers of flint nodules and becomes more massive at greater depths (Guillaume & Piau 2003). The microscopic observations of stone samples from the bedrock showed microcrystalline calcite matrix with fossils and quartz grains embedded in a micritic matrix (Marey Mahmoud 2010).

### **Research aims**

There are only few published data on the ancient materials used in the Pharaonic monuments at the western Thebes in comparison with the studies on the weathering mechanisms affecting these monuments. Because of this, this research was devoted to characterize samples of wall paintings collected from the tomb of *Djehutyemhab* (TT194), (Ramesside Period, c. 1298–1064 BC), El-Qurna necropolis (Luxor), Upper Egypt. The analytical techniques utilized in this work were optical microscopy (OM), scanning electron microscopy (SEM) equipped with an energy dispersive X-ray detector (EDS), X-ray diffraction analysis (XRD), micro-Raman and Fourier transform infrared spectroscopies ( $\mu$ -Raman and FT-IR).

Microscopic methods are necessary for identification of the paint layers. From this technique, one can gather information on the sequence and stratigraphy of paint layers, colour and texture of those layers and their thickness (Silva 2006). Scanning electron microscopy has been extensively used for the material characterization of objects of artistic and archaeological importance, especially in combination with energy dispersive X-ray microanalysis (SEM/EDS) (Schreiner et al. 2004). XRD is considered the most famous method used in the identification of crystalline compounds by their diffraction. Raman spectroscopy is a micro-analytical technique with certain features which are extremely advantageous for applications in the field of art and archaeology. This technique is particularly suitable for the identification of pigments in complex matrixes and inorganic pigments in artworks (Edwards et al. 2000). Infrared spectroscopy is an analytical technique that provides information about the chemical bonding or molecular structure of materials, whether organic or inorganic (Christy 2001).

The results of this study might bring us much information on materials and technologies used during the Ramesside period in Egypt. Furthermore, the obtained results will be used in establishing a conservation plan of the tomb.

## **Materials and methods**

### **Sampling**

During the inspections of the studied tomb, the visual observations of the damaged wall paintings led to diagnose the weathering forms; the condition of the wall paintings has been unfortunately decayed extensively and varies considerably. As a result of these deterioration processes, a large number of detached fragments were found at the tomb. Also, representative very small pigment samples (a few milligrams) were carefully scraped off the painted walls with a metallic scalpel from areas showing a good state of preservation. The investigations were undertaken to gather mineralogical, spectroscopic and chemical data of the studied wall paintings.

### **Analytical techniques**

#### **Optical investigation (OM)**

In order to analyze the stratigraphy of the paint layers, polished cross-sections were prepared and examined. Tiny samples were embedded in epoxy resin (EpoFix), cross-sectioned using variable speed silicon carbide papers, and examined by a Zeiss (stemi DV4) stereomicroscope with Sony (DSC-S85) camera.

#### **Scanning electron microscopy (SEM-EDS)**

The morphology of the paint layers was investigated using a JEOL JSM-840A scanning electron microscope and the microanalysis was carried out using an energy dispersive X-ray detector (EDS) Oxford ISIS 300 micro analytical system, with a detection limit of less than 1% depending on the element. For matrix correction protocol, ZAF correction was used. Highly polished cross-sections prepared on the studied samples were examined using SEM. The investigation was carried out in the backscattered electrons mode (BSE), this mode usually provides more information than the secondary electron mode, thus the different grey range, a consequence of the atomic numbers of the elements constituent of materials, let us distinguish the different layers with different elemental composition.

#### **X-ray powder diffraction analysis (XRD)**

For the XRD measurements, the collected samples were ground into powder in an agate mortar. The measurements were performed using a Phillips PW1710 diffractometer with Ni-filtered  $\text{CuK}\alpha$  radiation on randomly oriented samples. The

samples were scanned over the 3–63° 2 $\theta$  interval at a scanning speed of 1.2°/min. Quantitative estimates of the abundance of the mineral phases were derived from the XRD data, using the intensity of a certain reflection, the density and the mass absorption coefficient for CuK $\alpha$  radiation for the minerals present. Corrections were made using external standard mixtures of minerals. The detection limit was  $\pm 2$  % w/w.

#### $\mu$ -Raman spectroscopy

Micro-Raman spectra were recorded using a triple grating spectrometer (Dilor XY) equipped with a Charge Coupled Device (CCD) liquid-nitrogen cooled detector system. Raman spectra were recorded using the 632.8 nm excitation of an 35 mW air-cooled He–Ne laser (Spectra Physics, mod.127). The spectral resolution of the system was  $\sim 3$  cm $^{-1}$ . The laser was focused on the sample through the system's microscope equipped with a standard objective lens (100x). In order to avoid

damaging of samples, the laser power was kept at 0.1–0.3mW.

#### Fourier transform infrared spectroscopy (FT-IR)

Infrared spectroscopy is a powerful tool for analyzing both organic and inorganic materials, including crystalline and amorphous minerals. FT-IR spectra were collected using a Jasco 4200 FT-IR Spectrometer. Freshly prepared KBr pellets of powdered samples were prepared and examined in transmission mode in the wavenumber range of 4000–400 cm $^{-1}$ .

#### Results

The results of the semi-quantitative EDS microanalysis (atomic %) and the mineralogical composition determined by XRD method of the studied samples are given in **Tables 1. and 2.**, respectively.

**Table 1.: SEM-EDS microanalysis (atomic %) of the studied samples**

**1. táblázat: A vizsgált minták SEM-EDS vizsgálata – kémiai összetétel (atom %)**

Sample/ element	Na	Mg	Al	Si	S	P	K	Ca	Fe	Ti	Cu
Bedrock	–	–	3.58	4.60	1.4	–	–	41.66	–	–	–
	–	1.32	–	3.83	1.52	–	–	28.03	–	–	–
	–	2.23	2.43	4.87	0.97	–	–	31.27	–	–	–
Preparation layer	2.19	–	6.79	9.99	24.71	–	–	30.70	–	–	–
	–	–	9.74	7.42	5.39	–	–	27.37	–	–	–
	–	–	5.81	11.57	37.73	–	–	12.43	–	–	–
Blue pigment	10.09	2.39	5.47	45.22	18.46	3.69	1.5	19.08	1.84	–	4.19
	7.49	2.08	4.61	44.34	13.73	2.31	1.31	13.86	0.46	0.60	10.27
	5.85	1.52	2.22	39.52	14.59	2.03	1.45	19.05	1.27	–	21.75
Turquoise- green pigment	–	0.42	5.29	24.79	0.83	0.62	0.77	6.14	1.89	0.48	8.51
	–	1.81	4.95	13.37	4.10	0.46	1.01	6.53	1.13	–	6.68
	–	3.72	1.33	12.18	1.32	0.98	1.07	11.02	75.76	–	11.46
Red pigment	20.55	1.63	5.58	13.66	28.13	1.93	–	17.57	8.69	0.74	–
	11.81	2.06	10.32	21.01	17.04	3.00	–	16.18	15.61	1.29	–
	20.66	–	2.99	6.86	27.72	1.24	–	14.77	20.61	–	–
Yellow pigment	1.99	–	10.57	47.18	14.80	–	2.80	9.33	8.10	2.57	–
	0.72	–	14.09	27.91	7.65	–	0.87	18.21	11.53	1.09	–
	–	–	8.79	18.62	8.73	–	–	12.83	2.64	0.28	–

**Table 2.:** The mineralogical composition of the studied samples**2. táblázat:** A vizsgált minták ásványos összetétele

Sample/Component	C	Q	An	Gy	Pl	EB	Wol	He	Go	Ha	Cl
Bedrock	+++	++	+	-	-	-	-	-	-	+	+
Preparation layer	++	+	++	+++	-	-	-	-	-	+	+
Blue pigment	+++	+	+++	++	-	+	-	-	-	-	-
Turquoise-green pigment	++	+++	+++	+++	-	-	++	-	-	-	-
Red pigment	++	+++	-	++	+	-	-	+	-	-	+
Yellow pigment	+++	-	++	+++	+	-	-	-	+	-	+

C= calcite; Q=quartz; An=anhydrite; Gy=gypsum; Pl= plagioclase; EB=Egyptian blue; Wol=wollastonite; He= hematite; Go= goethite; Ha=halite; Cl=clay minerals, - = not determined; + = traces; ++ = minor constituent; +++ = major constituent.

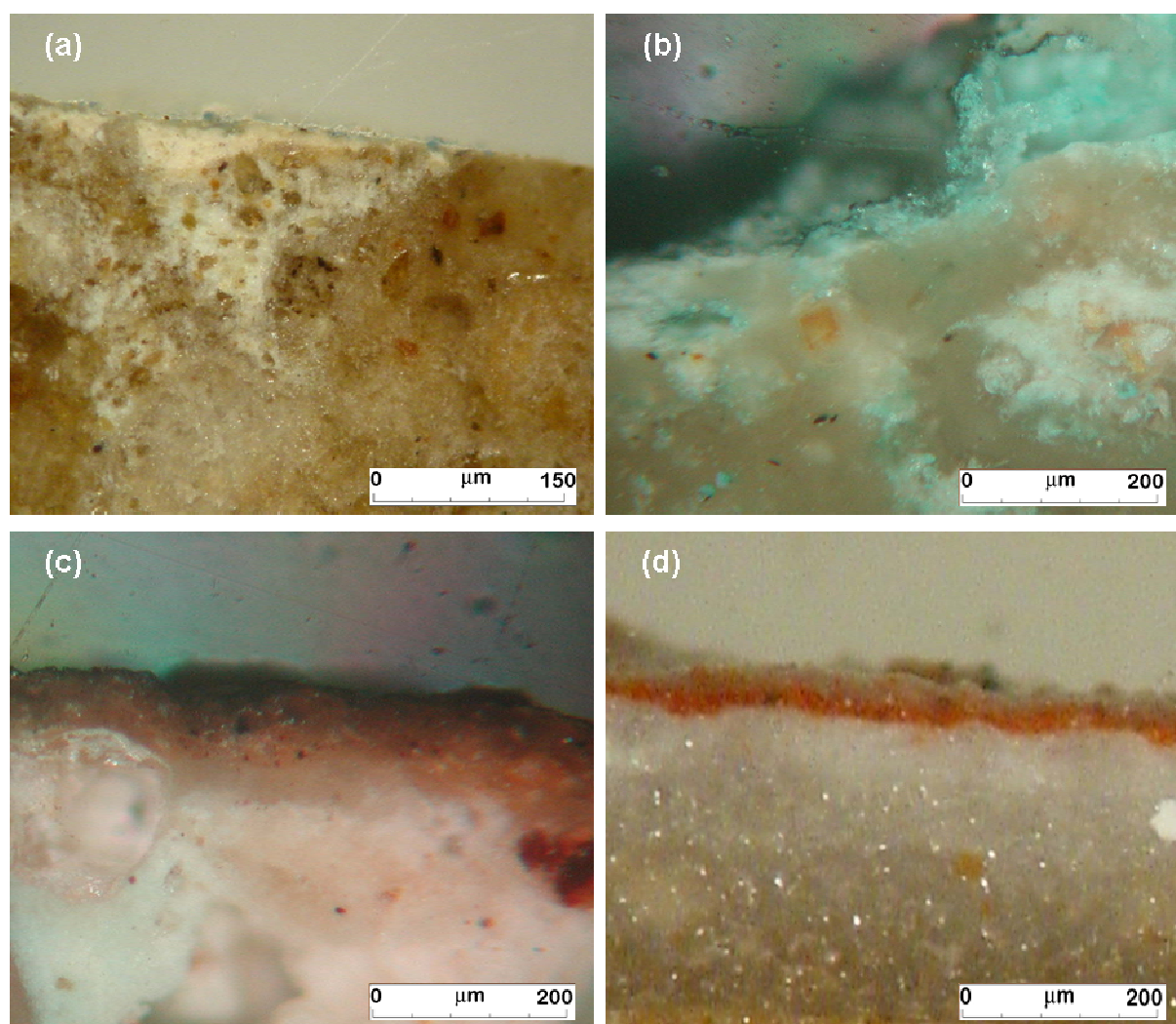


**Fig. 1.:** Optical photomicrographs of cross-sections of the paint layers. (a) The blue paint layer (microscope objective 10x magnification). (b) The turquoise-green paint layer (microscope objective 20x magnification, under reflected light). (c) The yellow-orange paint layer (microscope objective 20x magnification, under reflected light). (d) The red paint layer (microscope objective 20x magnification).

**1. ábra:** Mikroszkópos felvételek a festékrétegekről (a) kék festék (b) türkiz zöld festék. (c) sárga, narancssárga festék. (d) vörös festék

### Optical examination

**Figure 1.** illustrates the optical photomicrographs obtained on the examined paint layers. In respect with the optical observation of the stratigraphic structure of the paint layers, it was clear that the paints are applied on a thin layer of the white preparation layer. In some areas of the wall, however, the paints were applied directly on the well-polished stone substrate. In the case of the blue paint layer, we can observe tiny particles of the blue pigment are scattered on a thin white wash (ranging from 100 to 200  $\mu\text{m}$ ) (**Fig. 1a**). The optical examination of the turquoise-green paint layer (**Fig. 1b**) shows that this layer is slightly thick and the colour of the sample is a brilliant turquoise, which suggests that the pigment has been produced in an oxidizing atmosphere. Different firing temperatures and cooling rates create a large range of hues (Marey Mahmoud 2004). The optical examination of the red pictorial layer (**Fig. 1c**) shows a thin red irregular layer with dark particles diffusing into the layer. In the case of the yellow

pictorial layer, the optical examination shows orange-yellow hues and a dark film covers the paint layer (**Fig. 1d**). Moreover, in most of the cross-sections we can observe that the stone substrate below the paint layers is rich in large grains of quartz.

### BSE-EDS results

The backscattered electrons images (BSE) obtained on the outer surface of the studied samples are given in **Figure 2**. The microanalysis of the blue paint layer revealed as major elements silicon, calcium and copper, whose atomic percentage ratio are in agreement with the chemical formula of cuprorivaite ( $\text{CuCaSi}_4\text{O}_{10}$ ). The BSE image obtained on the blue paint layer (**Fig. 2a**) shows the heterogeneity and coarse crystals of cuprorivaite. Other elements like iron, sodium, potassium, titanium, aluminium, magnesium, sulphur and phosphorus were also detected. The presence of Ti in the studied samples could be a result of the presence of ilmenite ( $\text{FeTiO}_3$ ) which is found in the Egyptian sand (Berry 1999).

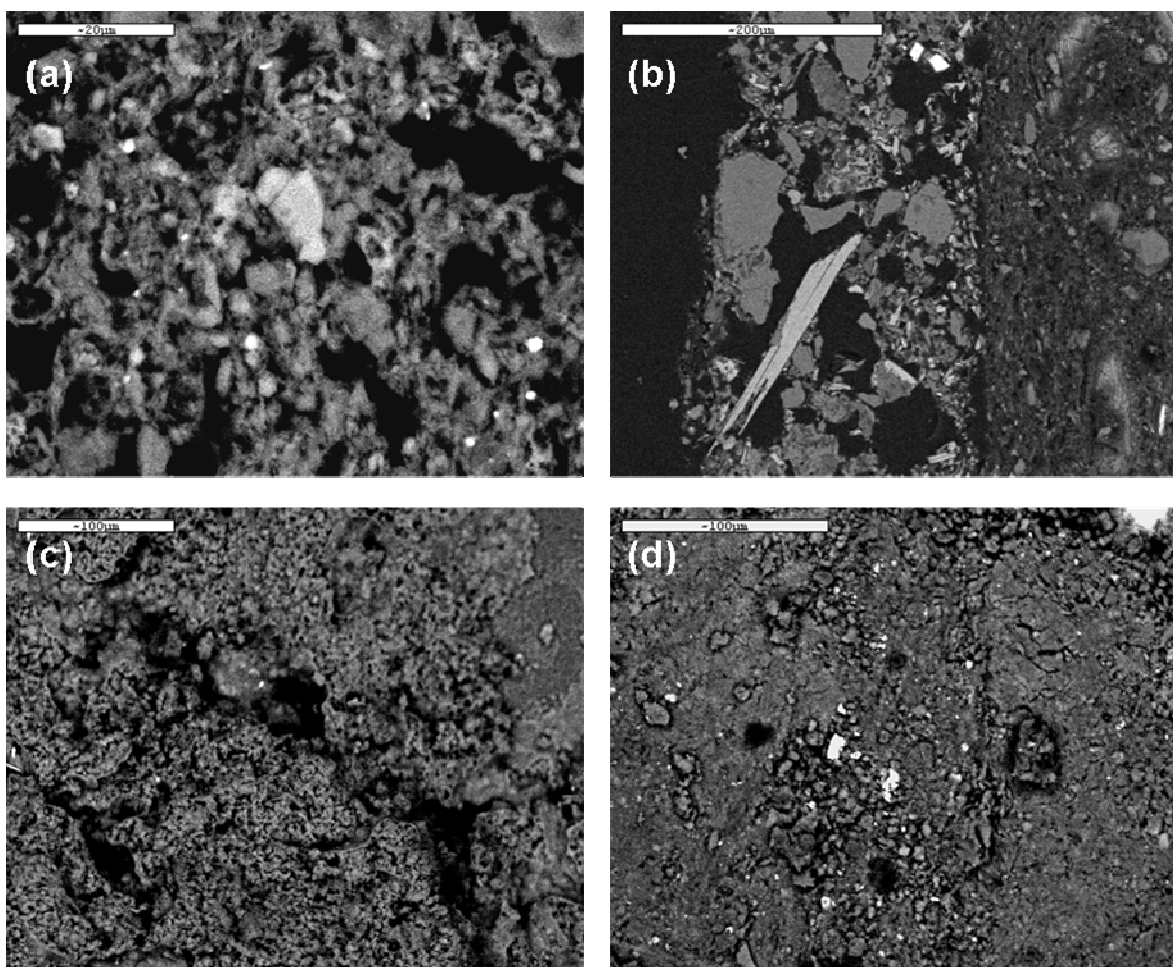


**Fig. 2.** BSE images obtained on the outer surfaces of the paint layers. (a) The blue paint layer. (b) The turquoise-green paint layer. (c) The red paint layer. (d) The orange-yellow paint layer.

**2. ábra:** Visszaszórt elektron kép (BSE) a festék rétegek külső felzínéről (a) kék festék (b) türkiz zöld festék. (c) sárga, narancssárga festék. (d) vörös festék

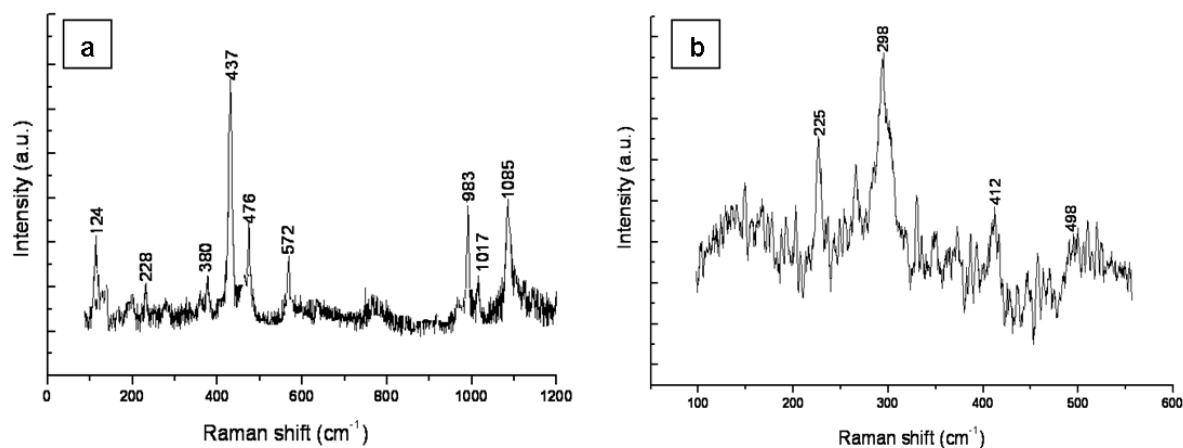


**Fig. 3.**  $\mu$ - Raman spectra recorded on pigment samples. (a) The blue paint layer. (b) The red paint layer.

**3. ábra:** A festékek  $\mu$ - Raman spektruma (a) kék festék (b) vörös festék

The microanalysis obtained on the turquoise-green paint layer revealed high ratios of silicon, while calcium and copper with other elements of aluminium, magnesium, potassium, sulphur, iron and phosphorus. BES image obtained on the sample shows a massive quartz, silica-rich amorphous phase and crystals of parawollastonite  $[(Ca,Cu)_3(Si_3O_9)]$  (**Fig. 2b**). EDS microanalysis of the red pictorial layer shows that the peak of iron (8–20%) is present, which indicates the existence of haematite ( $\alpha$ - $Fe_2O_3$ ) as possible colouring material. Sulphur and calcium detected in sample refer to the existence of calcium sulphates coming from the preparation layer. The strong contribution of aluminium and silicon indicates a possible existence of an aluminosilicate material (Zorba et al. 2007). BSE micrograph obtained on the sample shows the granular aggregate particles of the red ochre; large grains of gypsum are notable in comparison with the small ones of calcite from the preparation layer (**Fig. 2c**). The microanalysis of the yellow pigment sample, performed with EDS, shows the presence of iron (2–11%) indicating possible existence of goethite ( $\alpha$ - $FeOOH$ ). While the strong contribution of Al (27.64%) and Si (18–47%) indicates the existence of an aluminosilicate material (probably clay minerals); this indicates that yellow ochre was used to obtain the colour. BSE micrograph obtained on the sample shows the slightly small grains of the yellow ochre and calcite with large grains of gypsum scattered on the surface (**Fig. 2d**).

### Mineralogical characterization

XRD analysis of the stone substrate shows that calcite ( $CaCO_3$ ) is main crystalline phase in the sample. Minor amounts of anhydrite ( $CaSO_4$ ) and traces of halite ( $NaCl$ ) and clay minerals were also measured. XRD analysis of the preparation layer samples indicates the presence of gypsum

( $CaSO_4 \cdot 2H_2O$ ) as the predominant phase in the sample. Minor amounts of anhydrite and calcite were determined. Traces of quartz ( $SiO_2$ ), halite and clay minerals were also measured. XRD analysis of the blue paint layer shows that it consists mainly of calcite and anhydrite with minor amounts of gypsum and traces of quartz and cuprorivaite. XRD analysis of the turquoise-green pigment shows that it consists mainly of quartz, anhydrite, gypsum and secondary components of calcite and parawollastonite with traces of the mineral cuprorivaite. XRD measurements of the red pigment sample showed that quartz is the main component; with minor amounts of calcite and gypsum. Traces of haematite, plagioclase ( $NaAlSi_3O_8$ ) and clay minerals were also determined. In the case of the yellow paint layer, XRD measurements show that the sample consists of calcite, gypsum, with minor amounts of anhydrite and traces of plagioclase, goethite and clay minerals.

### $\mu$ -Raman results

Micro-Raman spectroscopy was used as a complementary technique to analyze some pigment samples. **Figure 3** shows the Raman spectra collected on the blue and red paint layers. Raman spectrum collected on a blue crystal from the blue paint layer reveals the identification of Egyptian blue through the characteristic bands at 1085, 1017, 983, 572, 472, 437, 476, 380, 228 and 124  $cm^{-1}$  (**Fig. 3a**). The band at 1084  $cm^{-1}$  (symmetric  $CO_3^{2-}$  stretching,  $\nu_1$ ), is attributed to calcite ( $CaCO_3$ ) probably coming from the preparation layer below. The bands at 200 and 400  $cm^{-1}$  are probably due to the presence of quartz.  $\mu$ -Raman analysis of the red pigment sample (**Fig. 3b**) shows the main characteristic strong bands at 225, 298, 412 and 498  $cm^{-1}$  which can be assigned to haematite.

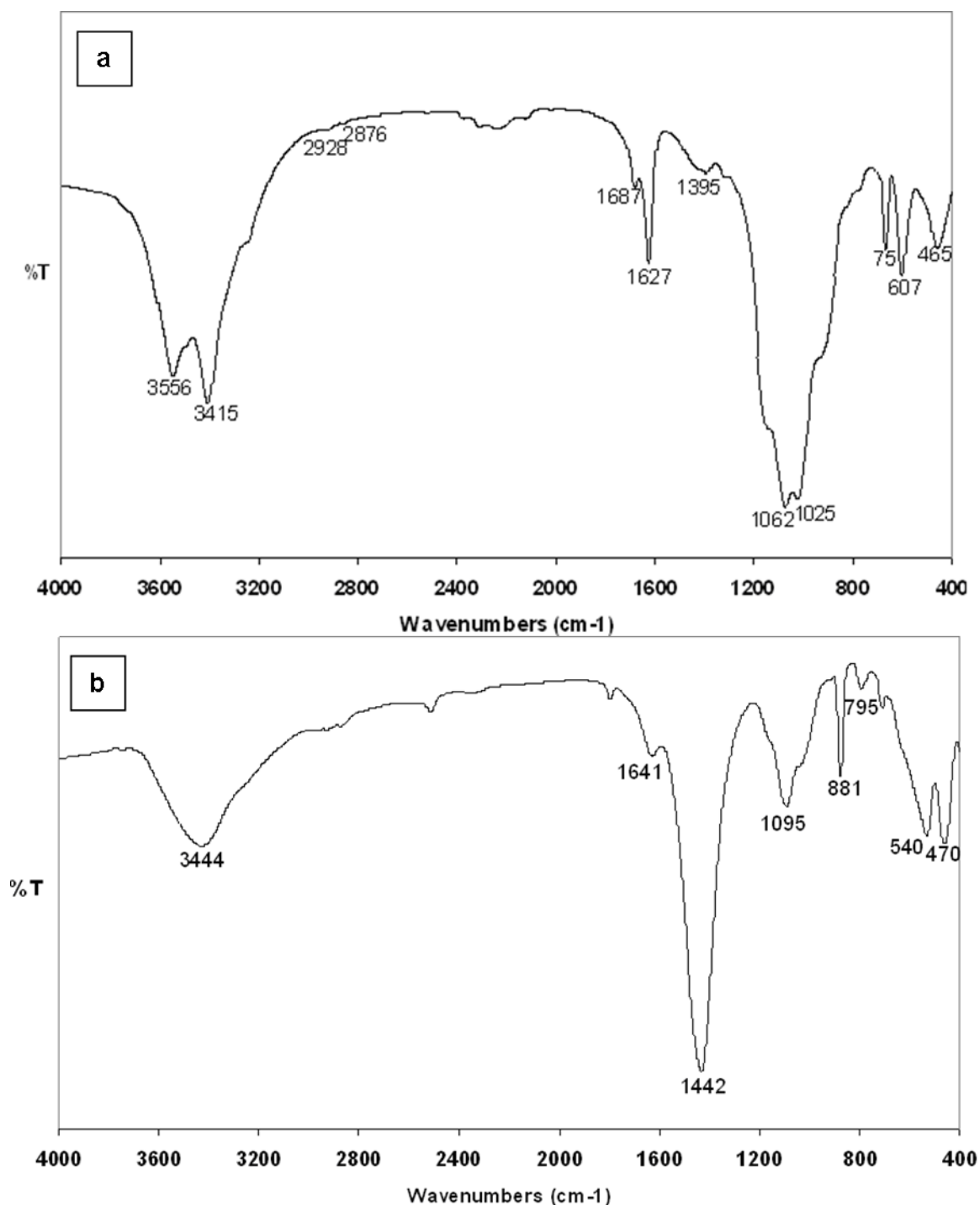


**Fig. 4.** Transmission FT-IR spectra (in KBr pellet) of pigment samples. (a) The blue paint layer. (b) The red paint layer.

**4. ábra:** FT-IR spektrumok a festékmintákról (KBr pelletben vizsgálva) (a) kék festék (b) vörös festék

#### FT-IR results

**Figure 4** displays the FT-IR spectra obtained on samples of the attested pigments. FT-IR spectrum (**Fig. 4a**) of the blue pigment sample presents characteristic bands lying mainly between 1280 and 1000  $\text{cm}^{-1}$  that are attributed to Si-O-Si stretching vibrations. The intense bands at 1025 and 1062

$\text{cm}^{-1}$  and the one at 1144  $\text{cm}^{-1}$  are all of the Egyptian blue. In the FT-IR spectrum (**Fig. 4b**) of the red pigment sample the band at 540  $\text{cm}^{-1}$  indicates the presence of iron oxide (haematite), the bands at 1442 and 715  $\text{cm}^{-1}$  are attributed to calcite and the band at 1641  $\text{cm}^{-1}$  is attributed to gypsum. The bands at 1095, 881 and 800  $\text{cm}^{-1}$  are attributed

to Si–O–Si and Si–O stretchings. The FT–IR spectrum collected on the yellow pigment (not shown) shows bands at 797 and 902  $\text{cm}^{-1}$  assigned to the vibrational modes of goethite.

It is sometimes difficult to differentiate these bands from the corresponding ones for stretching Si–O situated in the range 900–1100  $\text{cm}^{-1}$ , if they are accompanied of silicates (ochres) (Franquelo et al. 2009). The band at 1452  $\text{cm}^{-1}$  is attributed to calcite, and the band at 1629  $\text{cm}^{-1}$  is attributed to gypsum. The bands at 1083 and 1032  $\text{cm}^{-1}$  are attributed to (Si–O) stretching; the bands at ~400 and 463  $\text{cm}^{-1}$  indicate the presence of amorphous silicates. The band at ~3430  $\text{cm}^{-1}$  is due to free hydroxyl ions of kaolinite, bands of water H–O–H str., and a broad band at ~3140  $\text{cm}^{-1}$  was attributed to –OH stretching of hydrated ferric oxide. The use of proteinaceous binder (e.g. animal glue) was revealed on the bands at 1520–1560 ( $\text{NH}_2$ ) and 3284  $\text{cm}^{-1}$  ( $\nu\text{N–H}$ ), methylenic groups at ~2919 and 2851  $\text{cm}^{-1}$  ( $\nu_{\text{asym}}$  and  $\nu_{\text{sym}}\text{CH}_2$ ) and the band at 1657  $\text{cm}^{-1}$  for amide I ( $\nu\text{C=O}$ ) and 1538  $\text{cm}^{-1}$  for amide II (mainly  $\delta\text{N–H}$ ).

## Discussion

### Paintings support (bedrock)

XRD data showed that the main crystalline phases found in the limestone samples are calcite, quartz, anhydrite, halite and clay minerals. According to Marey Mahmoud (2010), the limestone types of the Theban Mountain belong to microsparry calcite embedded in a micrite matrix rich in fossils and grains of quartz.

### Preparation layer

The majority of the examined paint layers were applied on a thin preparation layer. The thickness of this layer ranges from 100 to 250  $\mu\text{m}$ . EDS microanalysis of this layers revealed the presence of calcium and sulphur as main elements in the preparation layer. Indeed, XRD analysis showed that a mixture of gypsum and calcite were used in the preparation layers.

### Blue pigment

By XRD, FT–IR and  $\mu$ -Raman analyses the blue pigment was identified as Egyptian blue. The microanalysis revealed the presence of copper, calcium and silicon as predominant elements with traces of iron, potassium, titanium, aluminium, magnesium, sulphur and phosphorus. Egyptian blue was the first synthetic pigment ever produced by man; this pigment appeared in Egypt during the 3rd millennium BC (Mirti et al. 1995). This pigment consists of cuprorivaite with variable amounts of wollastonite ( $\text{CaSiO}_3$ ), Cu-rich glass and cuprite ( $\text{Cu}_2\text{O}$ ) or tenorite ( $\text{CuO}$ ) and was prepared by

melting the copper-rich ingredient with lime and desert sand (Jaksch et al. 1983).

### Turquoise-green pigment

The green pigment was identified as Egyptian green, a turquoise mineral substitute appeared shortly after the Egyptian blue and it has a similar elemental composition. Egyptian green is a multi-component pigment consisting of major green wollastonite, a blue copper-, sodium-and chlorine-bearing glass phase, sporadic cuprorivaite, silica minerals and the tin compounds cassiterite and malayaite (El Goresy 2000). EDS spectrum obtained on the sample showed high ratio of silicon probably due to the high amount of glass-bearing materials in the sample. XRD results showed that parawollastonite is present together with traces of cuprorivaite that give the possibility that Egyptian blue was added to the green pigment to produce a special hue.

### Red pigment

The red pigment was identified as red ochre. Elemental analysis on the red coloured layers revealed the detection of high amount of iron. Red ochre was used from the 5<sup>th</sup> Dynasty till the Roman times (Lee & Quirke 2000). The actual pigment is haematite, an iron (III)-oxide (Bikiaris et al. 1999; Ortega et al. 2001). Haematite is commonly present as a pigment in sediments having been subjected to weak diagenesis (e.g., red beds) and in some metamorphic rocks (Hradil et al. 2003).

### Yellow pigment

The yellow ochre was used to obtain the yellow colour in the tomb. Yellow ochre consists mainly of goethite mixed with clays, silicates and other minerals. EDS microanalysis performed on the sample revealed the presence of iron with aluminum and silicon, suggesting that iron oxides were used with aluminosilicates like kaolinite ( $\text{Al}_2\text{Si}_2\text{O}_5(\text{OH})_4$ ). Yellow ochre was widely used without interruptions from the 5<sup>th</sup> Dynasty (c. 2494–2345 BC) till the Roman period in Egypt (El Goresy et al. 1986). Goethite only uniquely occurs in nature in a pure form or as a massive mineral (Ortega et al. 2001; Hradil et al. 2003; Barnett et al. 2006). The hue of goethite is affected by its crystallinity and elemental purity.

## Conclusions

The examined wall paintings from the tomb of *Djehutyemhab* (TT194), (Ramesside Period, ca. 1298–1064 BC), El-Qurna necropolis (Luxor), Upper Egypt revealed a common chromatic palette widely used in ancient Egypt. Different analytical techniques like optical microscopy (OM), SEM–EDS, XRD,  $\mu$ -Raman and FT–IR spectroscopies were used for characterizing the

structure, morphology, chemical and mineralogical composition of the paint layers. The results indicated that calcite is the predominant phase found in the stone substrate with minor amounts of quartz and anhydrite with traces of halite and clay minerals. The main components of the preparation layer were identified as gypsum, anhydrite, and calcite. The blue pigment was identified as Egyptian blue (cuprorivaite,  $\text{CaCuSi}_4\text{O}_{10}$ ), the green pigment as Egyptian green (Cu-wollastonite) together with the mineral cuprorivaite, the red pigment was identified as red ochre (haematite,  $\alpha\text{-Fe}_2\text{O}_3$ ), the yellow pigment as yellow ochre (goethite,  $\alpha\text{-FeOOH}$ ). In summary, the results provided information about the painting materials and techniques used in ancient Egypt and particularly the Ramesside Period. Furthermore, the obtained results can be used in the conservation-restoration interventions of these murals.

### Acknowledgements

The author is grateful to Dr. Dimitrios Christofilos, Physics Divisions, School of Technology of Aristotle University of Thessaloniki, Greece for  $\mu$ -Raman analysis.

### References

- BARNETT, J.R., MILLER, S., PEARCE, E. (2006): Colour and art: A Brief History of Pigments, *Optic. Laser. Tech.*, **38**: 445–453.
- BERRY, M. (1999): A study of pigments from a Roman Egyptian shrine, *AICCM Bulletin*, 1–9.
- BIKIARIS, D., DANILIA SR., SOTIROPOULOU, S., KATSIMBIRI, O., PAVLIDOU, E., MOUTSATSOU, A.P. & CHRYSOULAKIS, Y. (1999): Ochre differentiation through micro-Raman and micro-FTIR Spectroscopes: application on wall paintings at Meteora and Mount Athos, Greece, *Spectrochimica Acta A* **56**: 3–18.
- CHRISTY, A.A., OZAKI, Y. & GREGORIOU, V.G. (2001): Modern Fourier Infrared Spectroscopy. In: BARCELO, D. (Ed.), *Comprehensive Analytical Chemistry*, Vol. **XXXV**, 131–194.
- EDWARDS, H.G.M., FARWELL, D.W., NEWTON, E.M., RULL PEREZ, F. & VILLAR, S.J. (2000): Raman spectroscopic studies of a 13th Century Polychrome statue: identification of a 'forgotten' pigment, *J. Raman Spectrosc.*, **31**: 407–413.
- EL GORESY, A., JAKSCH, H., ABDEL RAZEK, M. & WEINER, K.L. (1986): *Ancient pigments in wall paintings of Egyptian tombs and temples: an archaeometric project*, Preprint of the Max Planck Institute of Nuclear Physics MPI H- V 12, Heidelberg.
- EL GORESY, A. (2000): Polychromatic Wall Painting Decorations in Monuments of Pharaonic Egypt: compositions, chronology and painting techniques. In: SHERRATT, S. (ed.), *Proceedings of the First International Symposium: "The Wall Paintings of Thera"*, Petros M. Nomikos and Thera Foundation, Piraeus, Athens, Hellas, **Vol. I**: 49–70.
- FRANQUELO, M.L., DURAN, A., HERRERA, L.K., JIMENEZ DE HARO, M.C. & PEREZ-RODRIGUEZ, J.L. (2009): Comparison between micro-Raman and micro-FTIR spectroscopy techniques for the characterization of pigments from Southern Spain Cultural Heritage. *J. Molecular Structure* **924–926**: 404–412.
- GUILAUME, A. & PIAU, J-M. (2003): Stability of the tomb of Rameses II (Valley of the Kings, Luxor, Egypt): Numerical models and reality, *Bulletin des Laboratoires des Ponts et Chaussées* **242**: 15–47.
- HRADIL, D., GRYGAR, T. & HRADILOVA, J. (2003): Clay and Iron Oxides Pigments in the History of Painting, *Applied Clay Science* **22**: 223–236.
- JAKSCH, H., SEIPEL, W., WEINER, K.L. & EL GORESY, A. (1983): Egyptian Blue-Cuprorivaite A Window to Ancient Egyptian Technology, *Naturwissenschaften* **70**: 525–535.
- KAMIL, J. (1976): *Luxor: A Guide to Ancient Thebes*, (2<sup>nd</sup> ed.), London. 138–141.
- KARL-JOACHIM, S (1995): Das Grab des Djehutiemhab (TT 194), Mainz am Rhein, Philipp von Zabern. 57-63.
- LEE, L. & QUIRKE, S. (2000): Painting materials. In: NICHOLSON, T.P and SHAW, I. (eds.), *Ancient Egyptian materials and Technology*, Cambridge University Press, 104–119.
- MAREY MAHMOUD, H.H. (2004): Scientific evaluation of treatment strategy of painted plaster layers applied on stone supports—applied on one of the New Kingdom Nobles tombs—Western bank, Luxor, *MSc. Thesis*, Department of conservation, Faculty of Archaeology, Cairo University.
- MAREY MAHMOUD, H.H. (2010): Archaeometric and petro-mineralogical remarks on damaged Egyptian wall paintings, El-Qurna necropolis, Upper Egypt, *Archeometriai Műhely* **7/2**: 149–156.
- MIRTI, P., APPOLONIA, L., CASOLI, A., FERRARI, R.P., LURENTI, E., AMISANO CANESI, A. & CHIARI, G. (1995): Spectrochemical and Structural Studies on a Roman Sample of Egyptian blue, *Spectrochimica Acta A* **51/3**: 437–446.
- ORTEGA, M., ASCENCIO, J.A., SAN-GERMÁN, C.M. & FERNÁNDEZ, M.E. (2001): Analysis of

Prehistoric Pigments from “Templo Mayor” of Mexico City, *J. Materials Science* **36**: 751–756.

PORTER, M & MOSS, R. (1960): Topographical Bibliography of Ancient Egyptian Hieroglyphic Text, Reliefs, and Paintings. I,1. The Theban Necropolis: Private Tombs. Oxford: Clarendon Press, pp. 353–355.

SCHREINER, M., FRÜHMANN, B., JEMBRIH-SIMBÜRGER, D. & LINKE, R. (2004): X-rays in art and archaeology: An overview, *Powder Diffraction* **19** (1): 3–11.

SILVA, C.L. (2006): A Technical Study of the Mural Paintings on the Interior Dome of the Capilla De La Virgen Del Rosario, Iglesia San José, San

Juan, Puerto Rico, MSc. thesis, University of Pennsylvania, USA.

WÜST, R.A.J. & SCHLÜCHTER, Ch. (2000): The Origin of Soluble Salts in Rocks of the Thebes Mountains, Egypt: The Damage Potential to Ancient Egyptian Wall Art, *J. Archaeological Science* **27** (12):1161–1172.

ZORBA, T., ANDRIKOPOULOS, K.S., PARASKEVOPOULOS, K.M., PAVLIDOU, E., POPKONSTANTINOV, K., KOSTOVA, R., PLATNYOV, V. & DANILLIA, SR. (2007): Infrared and Raman vibrational spectroscopies reveal the palette of frescos found in the medieval monastery of Karaach Teke, *Annali di Chimica* **97**: 491–503.